Microscopy and Microanalysis (2019), **25**, 1352–1366
doi:10.1017/S1431927619000448

Microscopy AND Microanalysis

Original Article

Effect of Ultra-Small Chitosan Nanoparticles Doped with Brimonidine on the Ultra-Structure of the Trabecular Meshwork of Glaucoma Patients

Indu Barwal[1], Rahul Kumar[1], Tanuj Dada[2] and Subhash Chandra Yadav[1]*

[1]Department of Anatomy, Nanotechnology Lab, Electron Microscope Facility, All India Institute of Medical Sciences, New Delhi 110029, India and [2]Dr. Rajendra Prasad Centre for Ophthalmic Sciences, All India Institute of Medical Sciences, New Delhi 110029, India

Abstract

Brimonidine, an anti-glaucoma medicine, acts as an adrenergic agonist which decreases the synthesis of aqueous humour and increases the amount of drainage through Schlemm's canal and trabecular meshwork, but shows dose-dependent (0.2% solution thrice daily) toxicity. To reduce the side effects and improve the efficacy, brimonidine was nanoencapsulated on ultra-small-sized chitosan nanoparticles (nanobrimonidine) (28 ± 4 nm) with 39% encapsulation efficiency, monodispersity, freeze–thawing capability, storage stability, and 2% drug loading capacity. This nanocomplex showed burst, half, and complete release at 0.5, 45, and 100 h, respectively. Nanobrimonidine did not show any *in vitro* toxicity and was taken up by caveolae-mediated endocytosis. The nanobrimonidine-treated trabeculectomy tissue of glaucoma patients showed better dilation of the trabecular meshwork under the electron microscope. This is direct evidence for better bioavailability of nanobrimonidine after topical administration. Thus, the developed nanobrimonidine has the potential to improve the efficacy, reduce dosage and frequency, and improve delivery to the anterior chamber of the eye.

Key words: brimonidine, glaucoma, nanobrimonidine, nanoencapsulation, ultra-small chitosan nanoparticles

(Received 2 September 2018; revised 5 March 2019; accepted 19 March 2019)

Introduction

Clinically recommended brimonidine, an α-adrenergic agonist, reduces intraocular pressure by decreasing aqueous humour production and increasing aqueous outflow in glaucoma patients (Cantor, 2006). However, due to poor bioavailability of brimonidine, higher doses (0.2% solution thrice a day) have been recommended to achieve therapeutic concentration. This leads to several side effects such as itching, stringing, blurring of vision, puffy eye, nausea, irregular heartbeat, shallow breathing, and numbness in the hands and feet (Bowman et al., 2004). To overcome these side effects, various formulations have been developed, but with limited improvement of brimonidine efficacy (Acheampong et al., 2002; De et al., 2003; Prabhu et al., 2010; Maiti et al., 2011; Yang et al., 2012; Natarajan et al., 2014; Kim et al., 2018; Newton & Rimple, 2018). Thus, it is important to enhance the ocular bioavailability and residence time in the anterior chamber to improve the functional efficacy of this drug (Mundada & Avari, 2009; Almeida, et al., 2013, 2014). Among the various reported methods, nanoencapsulation of brimonidine with compatible and biodegradable nanocarriers was reported to improve the efficacy for glaucoma patients (Prabhu et al., 2010; Aburahma & Mahmoud, 2011; Singh & Shinde, 2011; Yang et al., 2012; Ibrahim et al., 2015; Cho et al., 2016; Kim et al., 2018; Newton & Rimple, 2018). Biodegradable and biocompatible polymeric hydrogels and nanoparticles (NPs) were shown to prolong the residence time of brimonidine in contact with corneal tissue (Mundada & Avari, 2009; Almeida et al., 2013, 2014). In recent years, researchers have successfully developed various formulations based on *in situ* gelling systems, such as thermo-sensitive and pH-sensitive hydrogels (Acheampong et al., 2002; De et al., 2003; Prabhu et al., 2010; Maiti et al., 2011; Yang et al., 2012; Kim et al., 2018; Newton & Rimple, 2018). However, nanoencapsulation with mucosa adhesive chitosan NPs was reported to improve the efficacy of many drugs after topical administrations (De Campos et al., 2001; Alonso & Sanchez, 2003; Wu et al., 2005; Chen et al., 2007; de la Fuente et al., 2008; Motwani et al., 2008; Wang et al., 2008; Paolicelli et al., 2009; Aksungur et al., 2011; Luo et al., 2011). The major problem associated with chitosan NPs was the successful synthesis of ultra-small-sized NPs (<50 nm), which showed better penetration through the cornea to reach the posterior segment of the eye (Malhotra et al., 2009; Shang et al., 2014). These ultra-small chitosan NPs (US CS NPs) work as an ideal topical drug delivery vehicle because they resist washing by tears due to their mucosal adhesion. They are nontoxic, nonirritant, biodegradable and have the capacity of high drug loading, and slow but steady sustained release (Yadav et al., 2013; Sunkireddy et al., 2016). These US CS NPs of ~30 nm size showed better penetration in the cornea and other ocular barriers (Jarvinen et al., 1995; Sunkireddy et al., 2016).

*Author for correspondence: Subhash Chandra Yadav, E-mail: subhashmbu@gmail.com

Cite this article: Barwal I, Kumar R, Dada T, Yadav SC (2019) Effect of Ultra-Small Chitosan Nanoparticles Doped with Brimonidine on the Ultra-Structure of the Trabecular Meshwork of Glaucoma Patients. *Microsc Microanal* **25**, 1352–1366. doi:10.1017/S1431927619000448

We report the nanoencapsulation of the brimonidine on US CS NPs (termed as nanobrimonidine) by a cosynthesis method. Based on the work of Sunkireddy et al. (2016) the delivery of proteinaceous antioxidants to anterior and posterior chamber of the eye; the efficacy of brimonidine might be enhanced and this may open a new research for the other topically administered ocular drugs having dose-dependent side effects.

Materials and Methods

Materials

Low molecular weight chitosan (MW 50–190 kDa, 75–85% deacetylated, 448869), sodium tripolyphosphate (STPP), DMEM (Dulbecco's Modified Eagle's Medium) and pluronicF-68 (PF-68) were purchased from Sigma Aldrich (India). Milli Q water was purchased from Merck Millipore (India), glacial acetic acid from Fischer Scientific (USA), and phosphotungstic acid from Ted Pella, Inc (USA). DPBS (Dulbecco's Phosphate Buffer Saline), Pen–Strep (Penicillin and Streptomycin), and gentamycin were purchased from Life Technologies (USA). All other glassware and consumables were purchased from standard manufacturers.

Synthesis of Nanobrimonidine

Nanoencapsulation of brimonidine on US CS NPs (termed as nanobrimonidine) was performed by a modified ionotropic gelation process (Yadav et al., 2013). Briefly, low molecular weight chitosan polymer (225.0 mg) was dissolved in 100 mL of 1% acetic acid and sonicated for 2.0 h in a water bath sonicator at 20°C. The mechanical parameters, such as size of beaker (25.0 mL), size of magnetic bead ($1.0 \times 0.5 \times 0.5$ cm), height of final solution (1.0 cm), final volume of solution (15.0 mL), stirring speed (650 rpm), size of STPP drop (0.5 µl), and dropping rate (1.0 drop/s) were optimized as reported by our group (Yadav et al., 2013). Finally, 5.0 mL of aqueous STPP (2.0 mg/mL) containing 1.0 mg of brimonidine was added drop wise in 10.0 mL of chitosan solution (0.225%) at room temperature under constant stirring (650 rpm). The constituents were allowed to react under a similar stirring condition for 1 h after the completion of reactions. To prepare the naïve US CS NPs, only 5.0 mL of 2.0 mg/mL STPP solution was added drop wise in 10.0 mL of chitosan (0.225%) solution. All other parameters of synthesis were similar to nanobrimonidine as described above.

Stabilization and Isolation of Nanobrimonidine

Nanobrimonidine was capped with surfactants PF-68 by incubation. Aqueous solution (1.0 mL) of PF-68 (0.3% w/v) was added drop wise into nanobrimonidine suspension and capped for 15 min at room temperature under constant stirring. The resultant nanobrimonidine suspension was dialyzed quickly using a dialysis bag (cutoff 10.0 kDa) to remove the unreacted components. Nanobrimonidine (15 mL) was dialyzed using 30 mL dialysate (0.5% acetic acid) and 3.0 mL of the dialysate was concentrated to 1.0 mL for determination of encapsulation efficiency by an absorbance measurement. The synthesized nanobrimonidine was not separable by centrifugation. Thus, the dialyzed nanobrimonidine was concentrated by Amicon filter (10 kDa cutoff) and finally lyophilized using freeze drier.

Size Distribution and Zeta Potential Analysis

Nanobrimonidine (1.5 µg/mL of chitosan) and naïve US CS NPs (1.5 µg/mL) were diluted with 1% acetic acid, and sonicated in a bath sonicator for 5 min. Size distribution and zeta potential of synthesized NPs were analyzed by dynamic light scattering (DLS) using a Zetasizer (Malvern Instruments, Malvern, UK) equipped with 5 mW helium/neon laser. The experiments were performed at 25°C in triplicate. Scattered light was collected at an angle of 173° by a photon counting photomultiplier tube directed to a correlator to derive particle size from the correlator function.

Freeze-Drying and Redispersibility of Nanobrimonidine

Physical stability of nanobrimonidine NPs was assessed after 5 weeks. NPs were freeze-dried to study the stability of dried NPs and NP suspension after redispersion. Aliquots of 10 mL were frozen under liquid nitrogen and lyophilized. Freeze-dried samples were stored at room temperature, and rehydrated to original volume by adding filtered distilled water. Reconstituted samples were assessed for particle size, polydispersity index, and *in vitro* release.

Determination of Encapsulation Efficiency and Loading Efficiency

UV-visible absorption spectroscopy (at 246–319 nm) was used to measure the absorption of equal concentration of naïve ultrasmall chitosan and nanobrimonidine suspension. Amount of brimonidine encapsulated on US CS NPs was determined using a calibration curve. Standard concentrations of brimonidine were prepared and absorbance was measured at 246 and 319 nm to generate the calibration curve. Absorbance of equimolar concentration of brimonidine (70 µg/mL), similar concentration of naïve US CS NPs and nanobrimonidine (1.5 mg/mL of chitosan), three times concentrated dialysate as well as nanobrimonidine (using naïve chitosan 1.5 mg/mL as blank) was recorded on a Thermo Scientific Evolution 220 UV-Visible spectrophotometer. Encapsulation and loading efficiency of brimonidine on US CS NPs was calculated using the formula:

$$\text{Encapsulation Efficiency \%} = \frac{\text{Amount of encapsulated brimonidine}}{\text{Total amount of brimonidine used}} \times 100,$$

$$\text{Loading Efficiency \%} = \frac{\text{Amount of brimonidine in lyophilised formulation}}{\text{Total amount of nanobrimonidine}} \times 100.$$

Naïve chitosan and nanobrimonidine lyophilized powder were subjected to Fourier transform infrared (FTIR) spectra analysis. The FTIR spectra of lyophilized NP powder and pure brimonidine were recorded in the scanning range of 400–4000/cm.

In vitro *Release of Brimonidine from Nanobrimonidine Formulation*

Sustained release measurement was performed by re-suspending lyophilized nanobrimonidine from three reactions in 15 mL

phosphate buffer (0.1 M) with 0.5% acetic acid at pH 7.0. This was kept in a dialysis bag of cutoff 10 kDa and dialyzed in 30 mL resuspension buffer under stirred conditions. Samples from dialysate (1.0 mL) were collected at different time intervals (0–120 h) and absorbance was measured using resuspension buffer as blank. Percent release of brimonidine was calculated as per the formula:

$$\%\ \text{Release} = \frac{\text{Amount of brimonidine present in dialysate at time } t}{\text{Total amount of brimonidine in nanobrimonidine}} \times 100.$$

Transmission Electron Microscope Imaging

A small amount (0.2 mg) of lyophilized naïve chitosan NPs and nanobrimonidine powder was re-suspended in 1.0 mL acetic acid (1.0%) and sonicated for 20 min in a bath sonicator. One drop of sample was poured on 300-mesh carbon-coated copper grids and kept for drying at room temperature. These grids were negatively stained by uranyl acetate (1%) and dried before loading into the transmission electron microscope (TEM) for imaging. The actual size of NPs was measured in a high-resolution TEM (TECNAI, T20G2, TEM, FEI, Inc. Hillsborough, OR, USA) operated at 200 kV.

Assessment of Cellular Toxicity of Nanobrimonidine

L-929 cells were cultured in DMEM media supplemented with heat-inactivated (56°C, 0.5 h) 20% FBS. These cells were maintained at 37°C in a humidified atmosphere with 5% CO_2 and seeded onto 75 cm^2 culture flasks. Further, cells were harvested by a brief trypsinization (2 min). These trypsinized cells were seeded into 96-well plates (2×10^4 cells per well) for cell viability assays and *in vitro* uptake mechanism studies.

MTT assay was performed to evaluate the *in vitro* cytotoxicity of the nanobrimonidine on L-929 cells. Briefly, cells were seeded (2×10^4 cells/well) in 96-well plates and incubated for 24 h in a CO_2 incubator. Aliquots of the nanobrimonidine ranging from 10 to 5000 µg/mL (actual brimonidine concentration 0.2–100 µg/mL) were added to each well and incubated for another 24 h. Untreated cells were used as a control. After 24 h of incubation, 20 µl of MTT solution (5 mg/mL in DPBS) was added to each well and plates were incubated for another 2.0 h. MTT solution was then carefully removed and DMSO was added. The absorbance values were recorded using an ELISA microplate reader at 570 nm. Cell viability (%) was calculated according to the following equation:

$$\text{Cell viability (\%)} = \frac{\text{Absorbance of test sample}}{\text{Absorbance of control sample}} \times 100,$$

where the absorbance of a control sample is the absorbance for the control wells. All data were expressed as the mean of six measurements [mean ± SD (standard deviation), $n = 6$].

Cell Proliferation Assay

Cyquant assay was used to assess the L-929 cell proliferation study. These cells were treated with different concentrations of naïve chitosan NPs and nanobrimonidine (25, 50, 100, 200, 500, and 1000 µg/mL) for 24 h at 37°C. The cells were carefully washed with DPBS after removing the treatment media and placed at −70°C overnight to lyse. Cyquant GR dye along with lysis cell buffer was added to each well and incubated for 5 min at room temperature in dark place and fluorescence was measured at 520 nm.

In vitro *Time-Dependent Nanoparticle Uptake*

L-929 cells were seeded in Falcon™ six-well culture slides (2×10^6 cells/well) and incubated with rhodamine-labeled nanobrimonidine for 30 min, 1, 2, and 4 h. After the specified time, the media were removed and cells were washed thrice with 1× DPBS to remove the free NPs that were either not taken up or adhered on the cell surface. The cells were then trypsinized using 0.25% trypsin/EDTA and harvested by centrifugation at 1100 rpm for 5 min at room temperature. The cells were fixed with 4.0% paraformaldehyde (PF) for 20 min and sorted using FACS.

In vitro *Nanobrimonidine Uptake Mechanism*

Differentiated L-929 cells were seeded (2×10^4 cells per well) in a 96-well plate to determine the uptake mechanism of nanobrimonidine. These wells were pretreated with the endocytic inhibitors chlorpromazine (10 µg/mL, clathrin-mediated endocytosis), indomethacin (10.0 µg/mL, caveolae-mediated endocytosis), sodium azide (2 µg/mL), and colchicine (5 µg/mL, pinocytosis), respectively, for 1 h. Rhodamine-labeled nanobrimonidine (1 mg/mL) was incubated for 4 h. After treatment, the cells were washed with DPBS to remove free nanobrimonidine and lysed with 1% triton X-100 in 0.2 M NaOH. The resulting fluorescence was measured by exciting the sample at 530 nm and taking emission at 630 nm. The corresponding weight of the NPs was calculated from the standard graph plotted for rhodamine-labeled nanobrimonidine NPs.

Physiological Effect of Nanobrimonidine Treated Ex vivo *Trabeculectomy Tissue*

Freshly prepared sterile nanobrimonidine (10.0 mg/mL) equivalent to 0.2 mg/mL brimonidine was taken to determine the effect on trabecular meshwork opening of trabeculectomy samples. These samples were obtained from advanced glaucoma patients operated at Dr. Rajendra Prasad Center for Ophthalmic Sciences, All India Institute of Medical Sciences, New Delhi. Procedures conformed to the institute ethics committee resolution on the use of human samples for research before commencement of experiment. The transected trabecular meshwork tissue of glaucoma patients (total six patients) was incubated in DMEM media supplemented with heat-inactivated (56°C, 0.5 h) 20% FBS and antibiotics (1% Pen–Strep and gentamycin). In sterile conditions, the tissue of each patient was carefully dissected in DMEM into six parts, with trabecular meshwork in each part, under high-resolution dissection microscope. Two pieces were kept in fresh medium as controls, another two pieces were treated with 2.0 mg/mL brimonidine in medium and the remaining two pieces with nanobrimonidine (10 mg/mL) in medium (having brimonidine concentration 0.2 mg/mL) for 2 h at 37°C under suitable conditions. All these samples were individually fixed with modified Karnovsky's solution (glutaraldehyde 2.5%, PF 2.0% in 0.1 M phosphate buffer saline pH 7.4) for 5 h at room

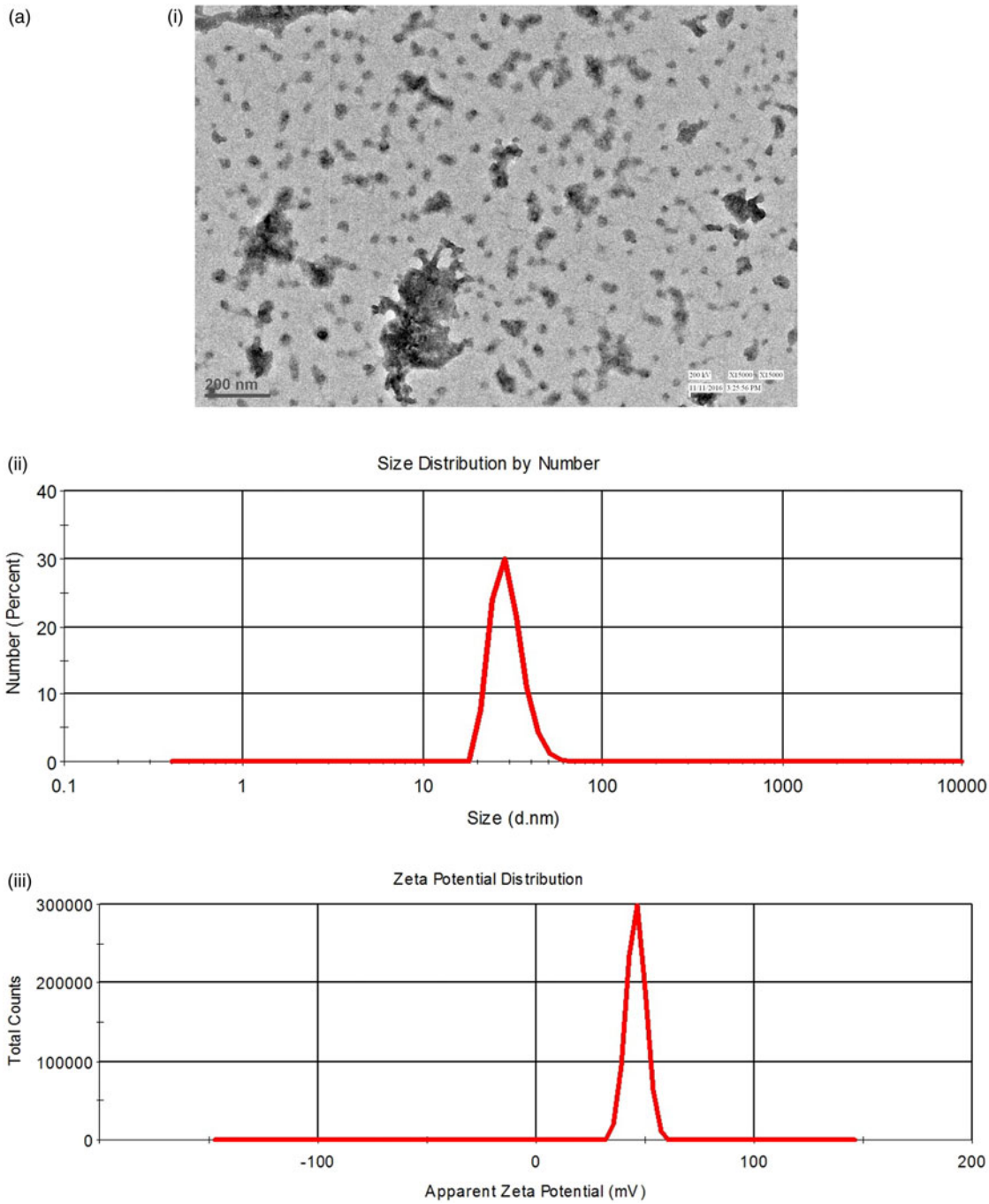

Fig. 1. Characterization of (**a**) ultra-small chitosan nanoparticles (naïve chitosan nanoparticles) and (**b**) nanobrimonidine (brimonidine encapsulated ultra-small chitosan nanoparticles): (i) TEM, (ii) size, and (iii) zeta potential of both nanoparticles synthesized by the modified mechanical-induced ionotropic gelation method. The TEM micrograph showed ultra-small, homogenous nanoparticles that were further confirmed by DLS analysis. TEM and DLS analysis revealed uniform size distribution with low PDI.

temperature and washed twice with DPBS. One sample of each condition (control, brimonidine, and nanobrimonidine treated) were serially dehydrated (from 10% acetone to 100% acetone, with 15 min interval and increment of 10% acetone), critical point dried (on EMS, K850), sputter coated with Au-Pd (on BARTEC, BU015331-T), and imaged in the scanning electron microscope (Zeiss, EVO 18, Oberkochen, Germany) operated at 20 kV. The remaining three samples of each patient were further fixed with 1% OsO_4 solution for 2 h at room temperature after removal of Karnovsky's solution. These samples were dehydrated, embedded in resin, ultra-sectioned (70 nm), stained with uranyl acetate (1%), and imaged in the TEM (Tecnai G20, FEI) operated at 200 kV.

Results and Discussion

Synthesis of Nanobrimonidine

Multiple combinations of the mechanical parameters of the ionotropic gelation method including sizes of reaction beaker

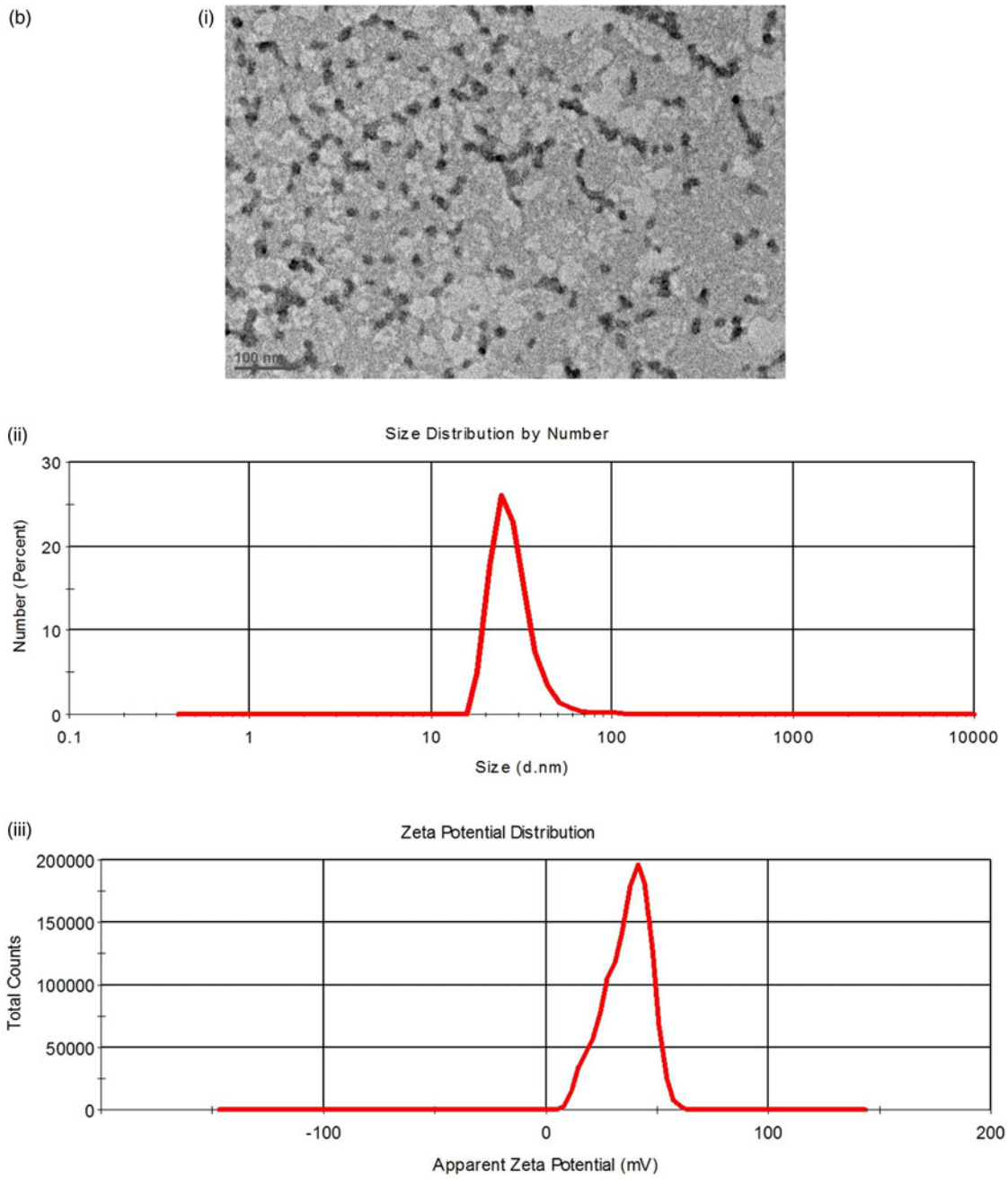

Fig. 1. Continued

(200–25 mL), final volume of NPs synthesis solution (50–15 mL), and maximum sizes of beads in relation to the reaction beaker size were standardized to synthesize nanobrimonidine. The effects of dropping speed (5–1 drop/s) and size of STPP drops (2.0–0.2 µl) were evaluated to explore these alterations on the size, monodispersity, and aggregation of the nanobrimonidine. The final optimized mechanical parameters such as beaker capacity (25 mL), final reaction volume (15 mL), rotation speed (650 rpm), magnetic bead size (1 × 0.5 cm), size of STPP drop (0.2 µl), and dropping rate (1.0 drop/s) were found to be optimum to synthesize ultra-small-sized nanobrimonidine (Fig. 1). These studies also emphasized the role of molar ratios of chitosan and STPP concentration (Fan et al., 2012) with optimized mechanical parameters. The changes in chitosan concentration (0.15–0.5% w/v) with fixed STPP concentrations (2.0 mg/mL) significantly altered the size of the US CS NPs (20 ± 5 to 500 ± 5 nm). Formation of chitosan NP aggregates (<0.15 or >0.5% w/v chitosan) was observed due to shift of equilibrium toward reduced biomolecular dynamic force. This equilibrium entirely depends on the concentration of chitosan, STPP, and their reaction volume ratio. The average size of NPs was decreased from 0.15 to 0.225% (w/v) and subsequently increased from 0.225 to 0.5% w/v chitosan (Supplementary Fig. 1). Increase in chitosan concentration above 0.225% w/v resulted in larger NP size due to an increase in hydrogen bonding and steric hindrance (reduce repulsion). However, the bigger particle size or aggregate formation below

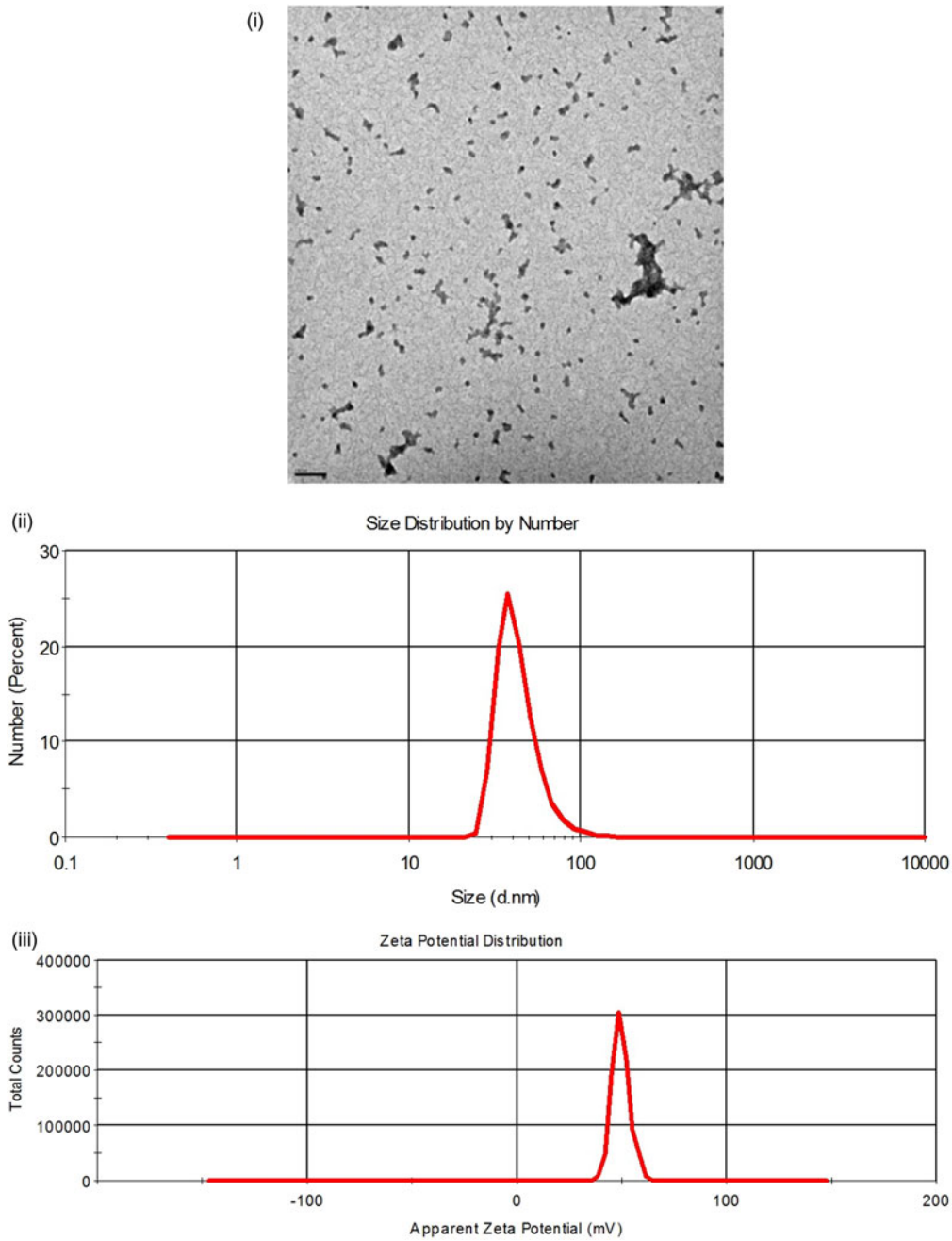

Fig. 2. Characterization of surface stabilized nanobrimonidine: (i) TEM, (ii) zeta size by DLS, and (iii) zeta potential of the PF-68-capped brimonidine-loaded chitosan nanoparticles. The PF-68-capped nanoparticles were highly stable due to better zeta potential. Scale bar: 100 nm.

0.225% chitosan was due to the increased intermolecular distances, elevated concentration of STPP (cross-linking density), less steric hindrance, and more Brownian movement between chitosan and STPP (Qun & Ajun, 2006). The pattern of our results is similar to that of reported by Calvo et al. (1997) and Fan et al. (2012), but our method synthesized US CS NPs. This again reflects the importance of mechanical parameters to synthesize such ultra-small NPs confirming the combined role of cross-linking agent (STPP) and optimum mechanical dynamic force to synthesize ultra-small-sized nanobrimonidine (Supplementary Figs. 2, 3). Similarly, with varied STPP concentration (constant chitosan 0.225% w/v and chitosan:STPP volume ratio 2:1) from 0.5 to 2.0 mg/mL, the size of chitosan NPs decreased from an average 100–25 nm. However, there was a sharp increase in size and aggregation at higher STPP concentration above 2.5 mg/mL (Supplementary Fig. 4). This could be attributed to the increase in molar ratio of STPP and chitosan, leading to a decrease in the intermolecular interaction. The size of chitosan NPs synthesized on varying the chitosan to STPP ratio (v/v) (chitosan 0.225% w/v and STPP 2.0 mg/mL) decreased on increasing the volume ratio from 1.75:1 to 2:1 (Supplementary Fig. 5). Thus, chitosan (0.225% w/v), STPP (2.0 mg/mL), and the volume ratio of chitosan:STPP solution (10:5 mL) were found to be optimum for the synthesis of monodispersed nanobrimonidine.

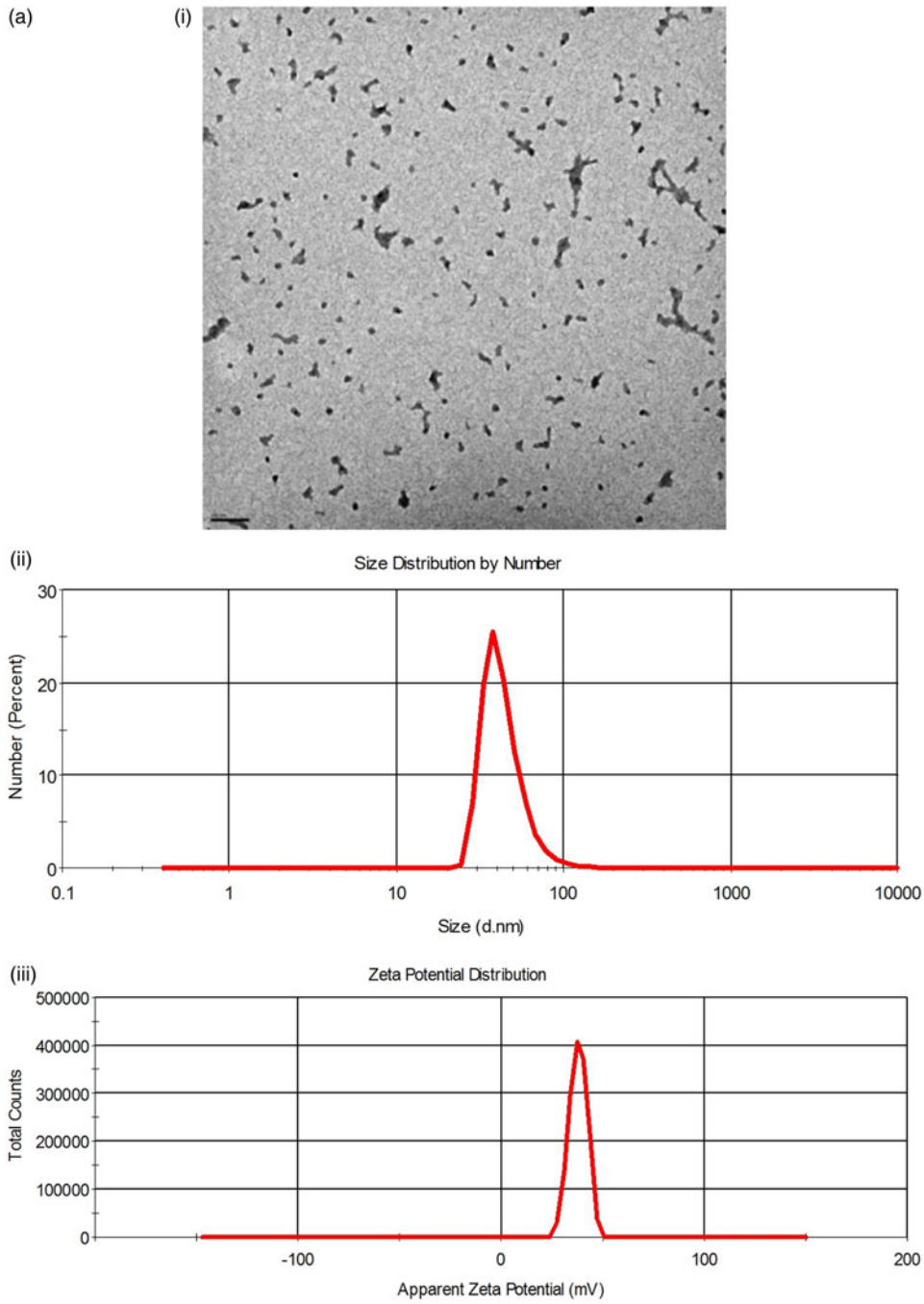

Fig. 3. Characterization of nanobrimonidine. **a**: One month storage without freeze-drying, (**b**) re-suspension after 2 days of freeze-drying and (**c**) resuspension 1 month after freeze-drying the sample. (i) TEM, (ii) zeta size by DLS, and (iii) zeta potential analysis. There is no change in morphology, size, and particle size distribution. Scale bar: 100 nm.

These mechanical and physicochemical parameters play a crucial role by providing the appropriate molecular dynamic energy from the mechanical energy. The stirring time was also found to be a crucial parameter for synthesizing nanobrimonidine. The best time to synthesize the smallest, homogeneous, stable nanobrimonidine was 1 h after the reaction because shorter (15 min) or longer (up to 24 h) stirring times produced larger size nanobrimonidine. The zeta potential of nanobrimonidine was not affected by stirring time (Supplementary Fig. 6). This was due to incubation-induced cross-linking rearrangement between chitosan and STPP, and further cross-linking between the synthesized US CS NPs. This further emphasizes that 1.0 h of stirring is ideal for the synthesis of US CS NPs in the current methodology. TEM images also proved that 1 h stirring was an ideal time for the reaction to synthesize ultra-small monodispersed nanobrimonidine NPs at the given conditions (Supplementary Fig. 6).

It has been reported that ultra-small-sized NPs showed better encapsulation of therapeutic drugs and better permeation and retention (EPR) in the ocular tissues (Shang et al., 2014;

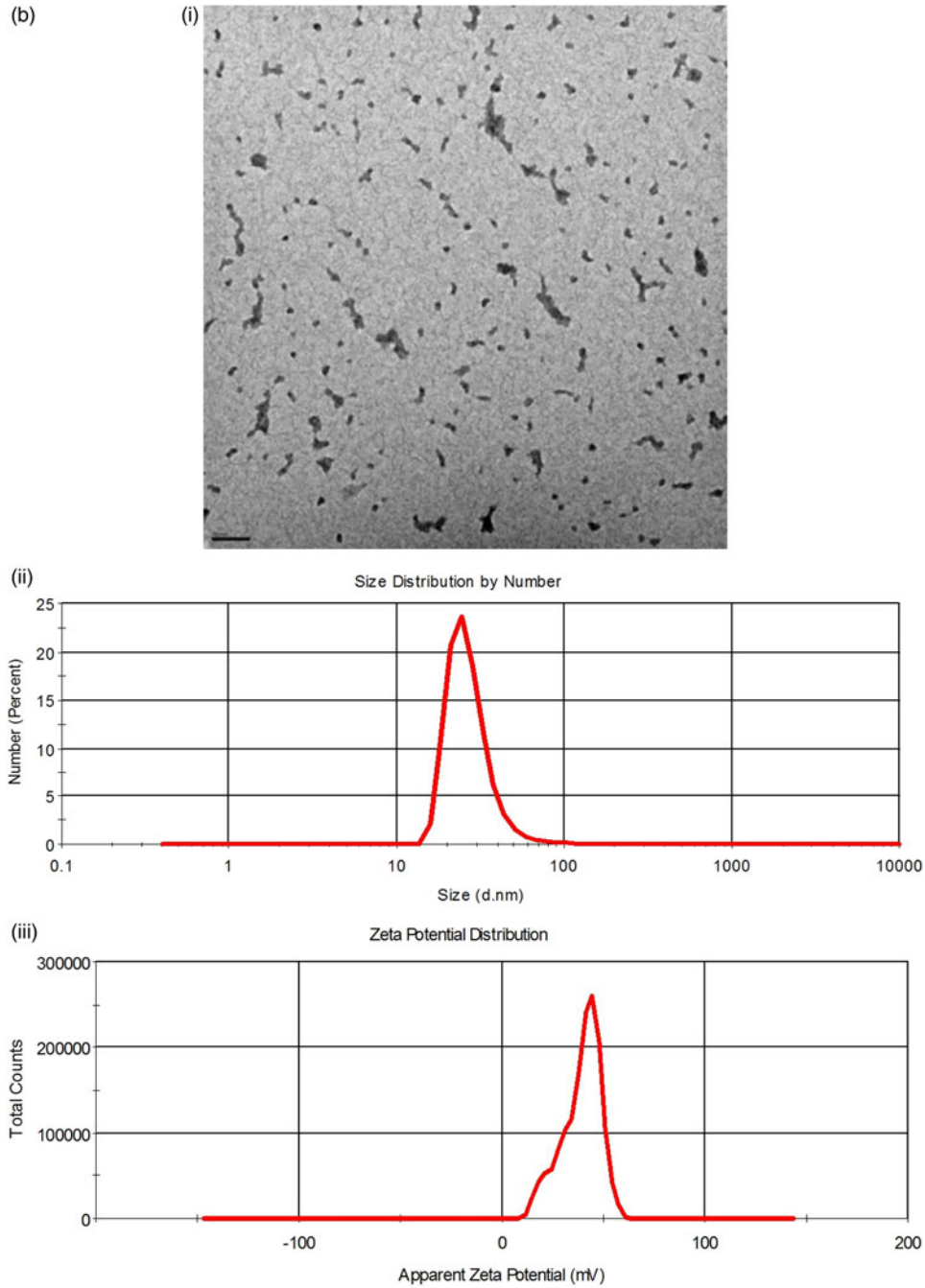

Fig. 3. Continued

Sunkireddy et al., 2016). These particles also showed effective intracellular delivery (easy tissue internalization) (Tallury et al., 2009), enhanced cellular uptake (Bonferoni et al., 2009), higher bioavailability and slow clearance by immune systems (longer half-life) in comparison to the larger sized chitosan NPs (>100 nm) (Hagens et al., 2007; Tallury et al., 2009; Shahrouz et al., 2014). Many efforts, such as chemical modification of chitosan (Banerjee et al., 2002; Chen et al., 2007; Elzatahry & Eldin, 2008; Tallury et al., 2009), applying complex synthesis processes (Wang et al., 2008; Santra, 2010; Santra & Tallury, 2011), and membrane-based synthesis using toxic organic solvents (Santra, 2010; Santra & Tallury, 2011), were made to synthesize US CS NPs. However, ultra-small (<30 nm) chitosan NP synthesis by simple and accessible methods with a high degree of homogeneity and stability has not been reported (Agnihotri et al., 2004; Fan et al., 2012). The mechanical parameters used in this report (to increase the molecular dynamic energy) shifted the equilibrium toward intermolecular hydrogen bond formation and electrostatic repulsion of the positively charged chitosan polymer. This equilibrium shift created a way to synthesize the US CS NPs by increasing the intermolecular distance, cross-linking density, and decreasing interparticle cross-linking.

Nanobrimonidine synthesized by this method showed a tendency to slow aggregation that also reduces the potentiality of

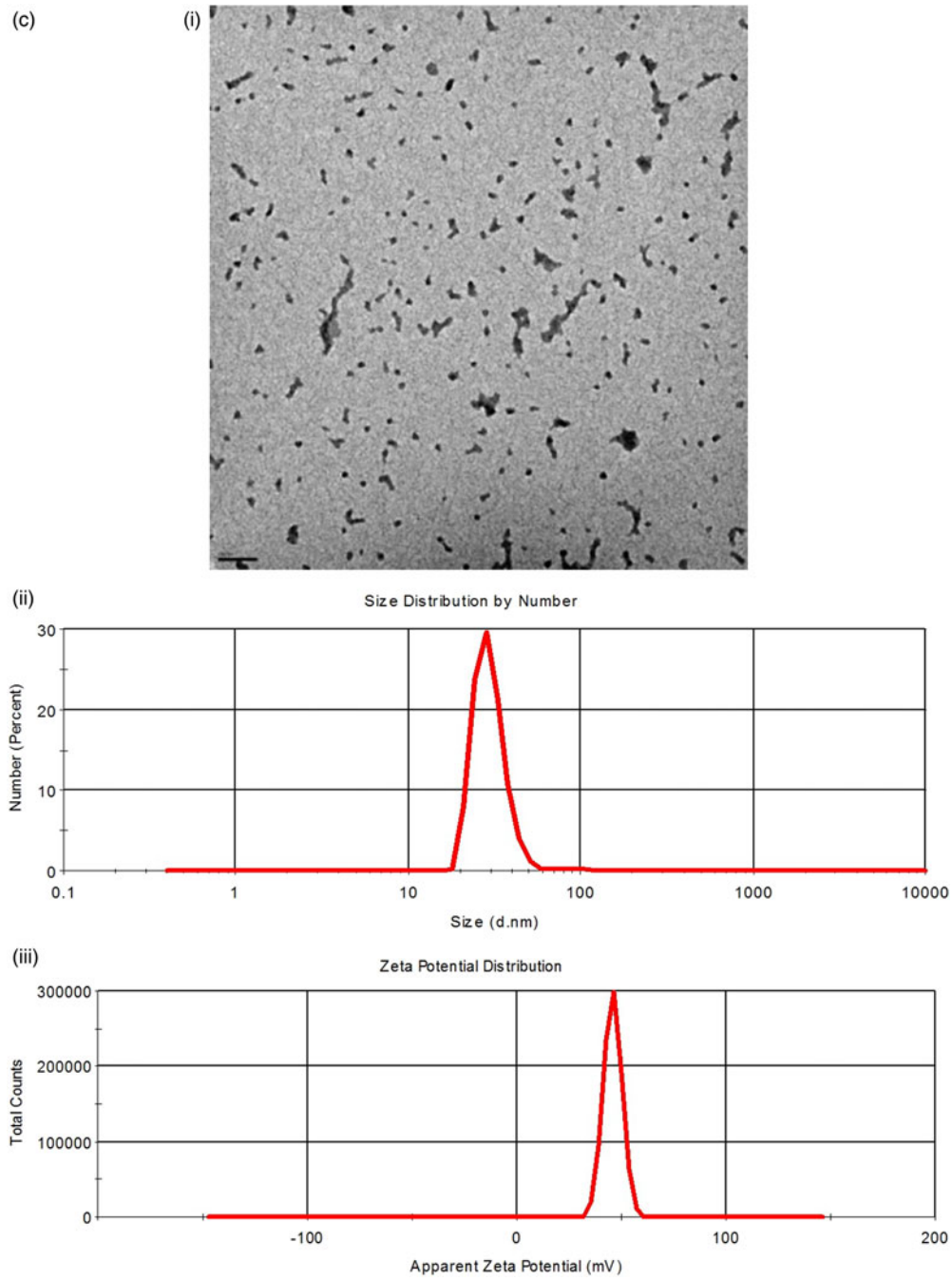

Fig. 3. Continued

long-term storage for commercial use. However, capping of nanobrimonidine with biodegradable and biocompatible surfactant PF-68 reduces the aggregation, improves the stability, and alters the surface charges. The zeta potential of PF-68-capped nanobrimonidine was increased from 32 to 38 mV (Fig. 2). Surfactant-capped NPs showed better stability as evident from the size distribution in TEM imaging. The average size and size distribution were decreased, whereas the zeta potential increased after capping with surfactants (Figs. 3a, 3b) (Anderberg et al., 1988; Binks & Lumsdon, 2001). This increased the storage stability of nanobrimonidine without altering the size (Fig. 3c). Similar results were also observed with naïve US CS NPs (Supplementary Fig. 7). Additionally, surfactant-capped nanobrimonidine showed better solubility from lyophilized powder and produced a homogeneous suspension (Fig. 3). The nanobrimonidine NPs did not separate from the suspension by centrifugation and even by ultracentrifugation up to 30,000 rpm. Hence, dialysis of diluted suspension followed by lyophilization was performed to isolate the nanobrimonidine. This method also reduced the loss up to 70% due to centrifugation-mediated aggregation (data not shown). The freeze-dried surfactant (PF-68)-capped nanobrimonidine showed similar size and zeta potential (Fig. 2). Thus, the dialysis and surfactant capping were effective to reduce the nanobrimonidine aggregation and maintain monodispersity as well as provided the stability of the suspension for long-term storage at room temperature.

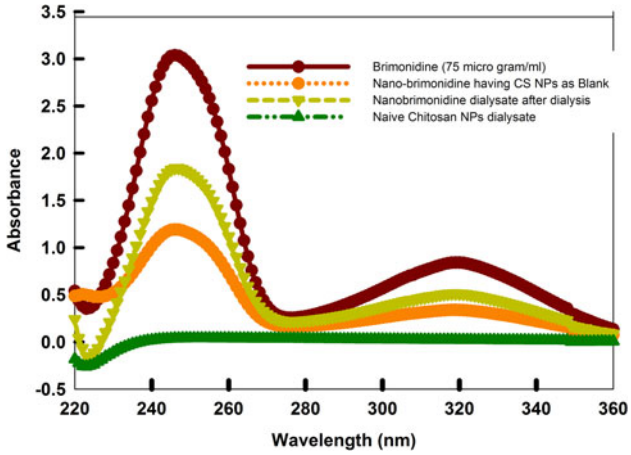

Fig. 4. UV-visible spectroscopic characterization of nanobrimonidine. UV-visible absorbance spectra of nanobrimonidine, chitosan, pure brimonidine (buffer as blank), and nanobrimonidine (chitosan as blank). Chitosan nanoparticles, chitosan nanoparticles dialysate, dialysate remained after chitosan nanoparticles dialysis, and pure brimonidine tartrate were used in the reactions [nanobrimonidine: brimonidine loaded ultra-small chitosan nanoparticles; nanobrimonidine dialysate: dialysate remained after dialysis of nanobrimonidine; nanobrimonidine using (CS NPs as blank): absorbance of nanobrimonidine nanoparticles using chitosan nanoparticles as blank].

Encapsulation Efficiency and Entrapment Efficiency

Encapsulation efficiency of brimonidine on nanobrimonidine was evaluated by UV-visible absorption spectroscopy using specific absorption peaks of brimonidine at 248 and 319 nm. The calibration curve was generated to estimate the drug encapsulation (Supplementary Fig. 8). The spectra of naïve US CS NPs showed no interference with brimonidine. The encapsulation efficiency was calculated by subtracting absorbance of initial brimonidine solution from dialysate (concentrated in a rotary evaporator). The encapsulation efficiency was also determined by recording the absorbance of isolated nanobrimonidine. An equal concentration of naïve US CS NPs was used as a blank. The amount of brimonidine encapsulated on nanobrimonidine was calculated with the help of a calibration curve from the resultant peaks at 248 and 319 nm (Fig. 4). Both results revealed that the encapsulation efficiency of brimonidine was 39 ± 3% (Supplementary Information 9). Nanobrimonidine showed monodispersity with a size distribution of 28 ± 4 nm and approximately 2.0% loading efficiency.

Encapsulation of brimonidine was also confirmed by FTIR spectroscopy using pure brimonidine, naïve US CS NPs and nanobrimonidine. Major characteristic peaks of the chitosan at 887, 1017, and 1068/cm were observed in both naïve US CS NPs and nanobrimonidine. The brimonidine peaks of NH bending at 1647/cm, and an aromatic nitro group at 1482 and 1530/cm were found in pure brimonidine and nanobrimonidine (Figs. 5a–5c). This gave a direct evidence of nanoencapsulation of brimonidine on US CS NPs (Fig. 5).

In vitro *Release*

An *in vitro* release study was performed using a dialysis bag of 10 kDa cutoff, because nanobrimonidine is impermeable and compatible with the dialysis membrane. The released amount of brimonidine in designated times was determined. It was found that 50% brimonidine was released within 45 h and completely released after 4 days using the cumulative drug release profile (Fig. 6). The result was taken from an average of three *in vitro* release experiments

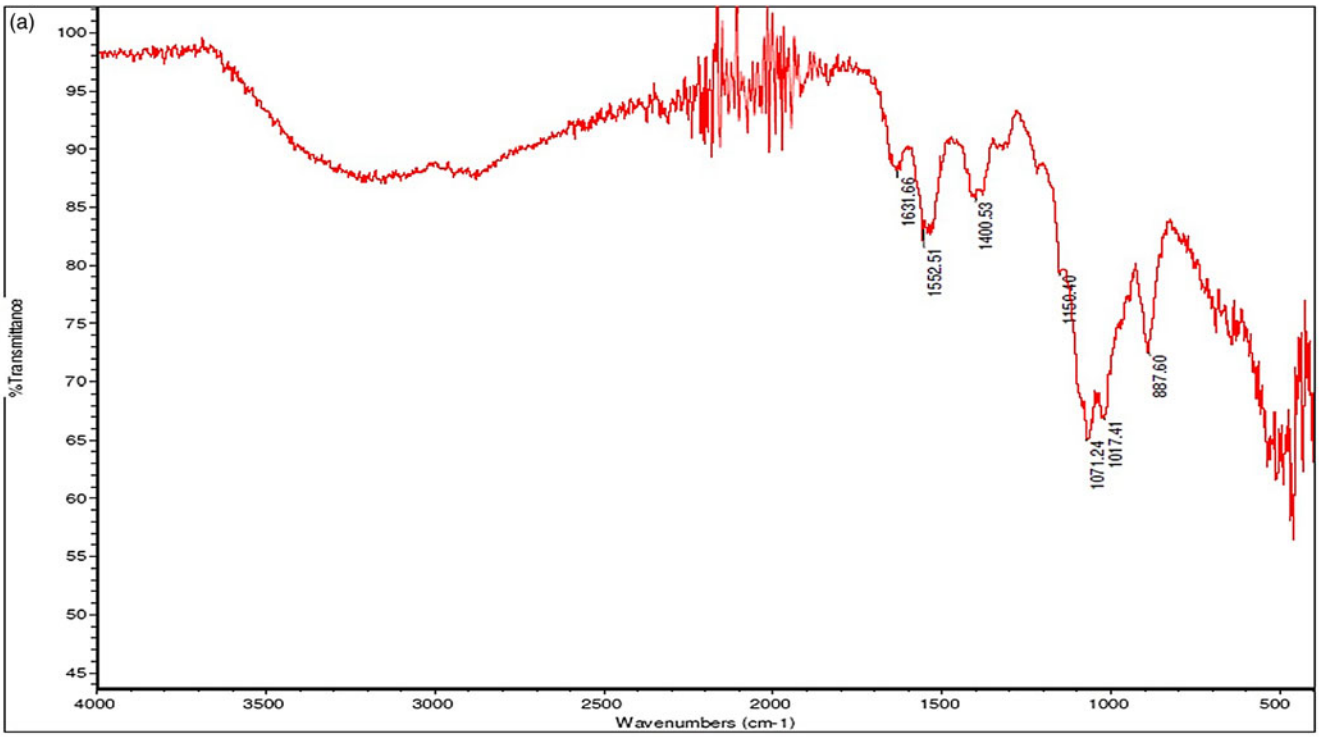

Fig. 5. FTIR spectra of (**a**) ultra-small chitosan nanoparticles (naïve chitosan nanoparticles), (**b**) brimonidine alone, (**c**) nanobrimonidine. Characteristic peaks for chitosan 887, 1017, 1068/cm were observed in both blank ultra-small chitosan nanoparticles and nanobrimonidine. The brimonidine peaks at 1647, 1482, and 1530/cm were found in pure brimonidine and nanobrimonidine.

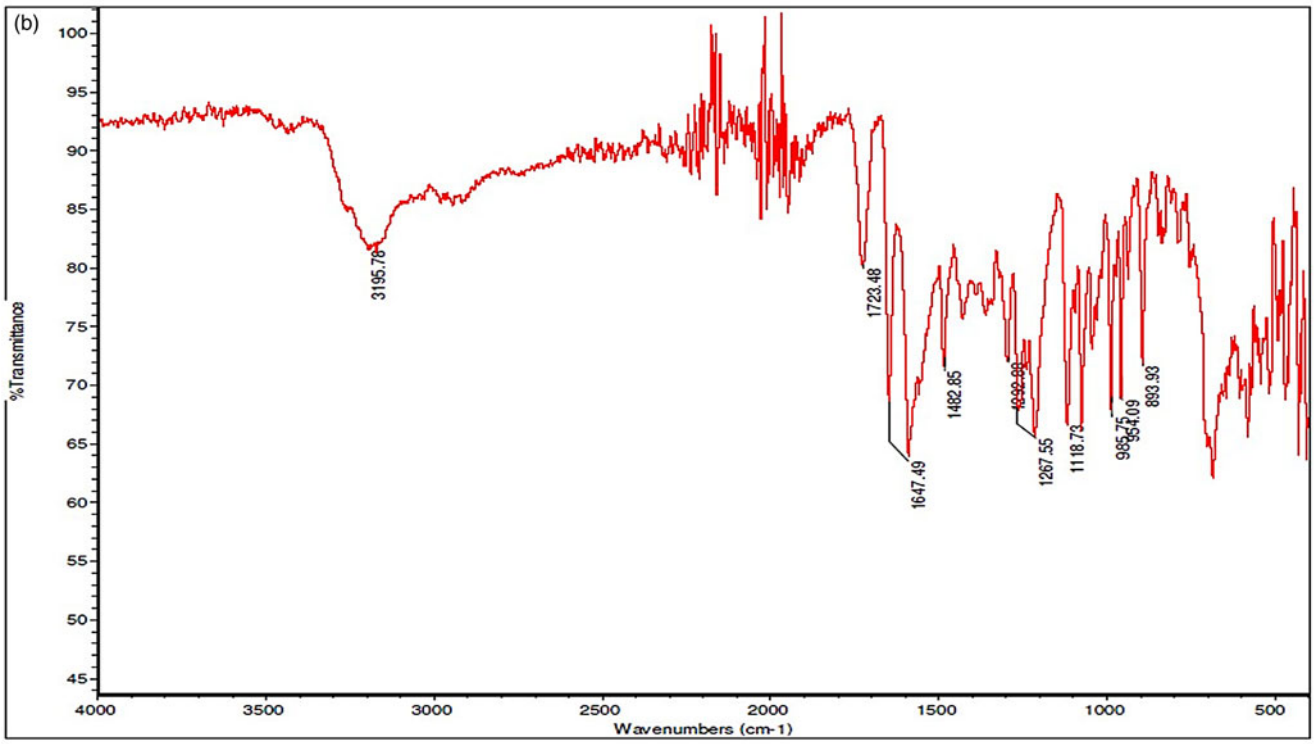

Fig. 5. Continued

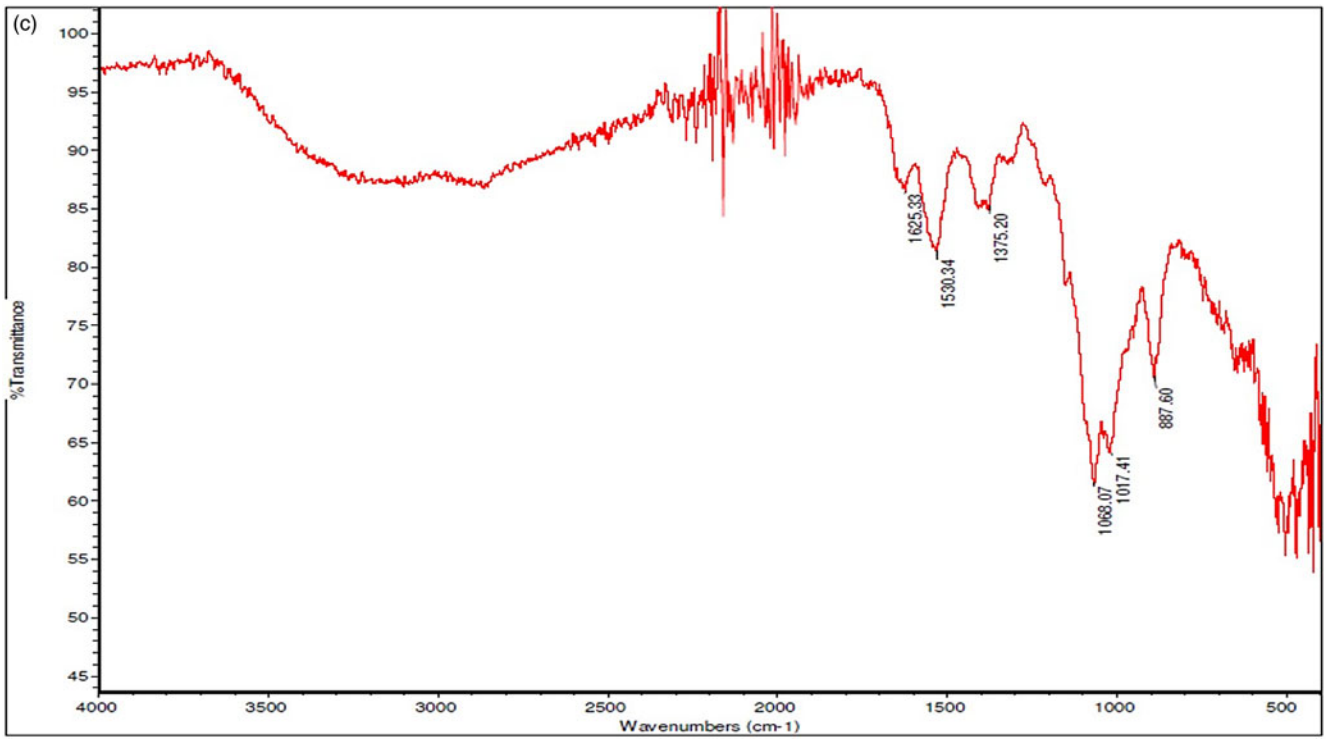

Fig. 5. Continued

(Supplementary Fig. 10). In another experiment to evaluate the mucosa-adhesive nature of nanobrimonidine, the cornea from a bull eye was treated with the rhodamine-labeled nanobrimonidine formulation. The treated cornea was gently washed with distilled water (1.0 mL/cm^2 area) for 10 min. Another nanobrimonidine-treated bull cornea was taken as a control. It was found that nearly 80% of nanobrimonidine was intact by fluorescence measurement (Supplementary Fig. 11). This was due to the ionic interaction

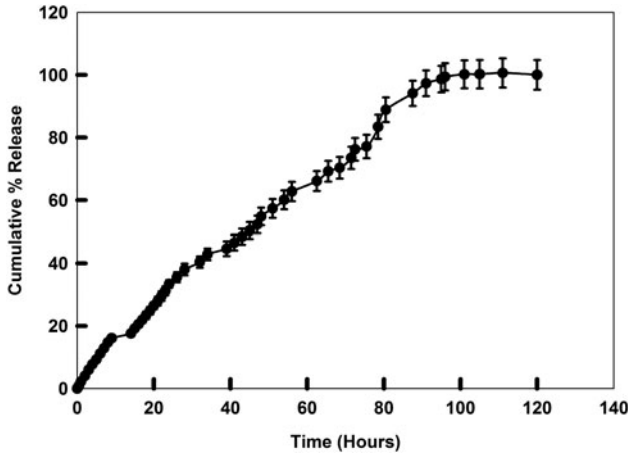

Fig. 6. *In vitro* release of brimonidine from nanobrimonidine at pH 7. There was half release of brimonidine at 45 h and sustained release up to 100 h. The nanobrimonidine synthesized from the three reactions were suspended in 15 mL, 0.5% acetic acid in phosphate buffer (0.05 M) at pH 7.4 and release was measured taking 1 mL from the dialysate (from 30 mL) having 0.5% acetic acid in phosphate buffer (0.05 M) at pH 7.4.

between positively charged amino groups of chitosan and negatively charged sialic acid residues in the mucous layer of the cornea (Lehr et al., 1992). Thus, nanobrimonidine has excellent mucosa adhesiveness with a prolonged retention period improving its permeability and sustained release. This property also increases the bioavailability of brimonidine and provides therapeutic efficacy at low concentration thus reducing the side effects.

Cellular Toxicity

The long-term goal of the current work is to improve the bioavailability and prolong the persistent time of brimonidine after topical administration. However, the toxicity due to prolonged exposure of nanobrimonidine needs to be established for patient safety. Though, many reports have shown that chitosan, as well as US CS NPs (Sunkireddy et al., 2016), are entirely safe for topical administration (de Campos et al., 2004; De Campos et al., 2001; Aksungur et al., 2011; Shi et al., 2015; Tang et al., 2014), in the context of cell membrane disruption by cationic NPs, we evaluated the cytotoxicity of nanobrimonidine on human lens epithelial cells (L-929). It was found that nanobrimonidine (up to 5 mg/mL)

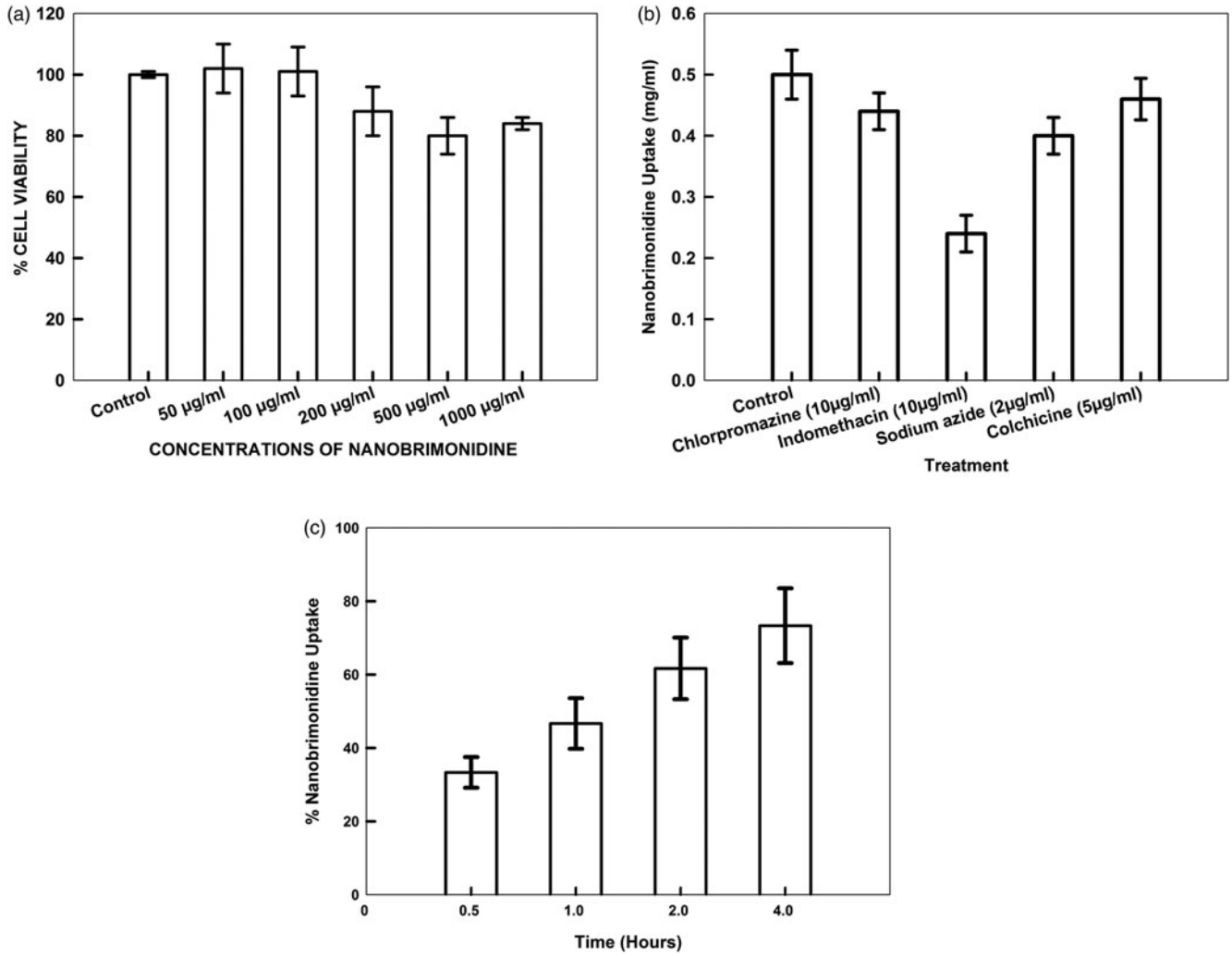

Fig. 7. *In vitro* analysis of nanobrimonidine. **a**: Cell viability assay: L-292 cells were used to measure the viability applying various concentrations of nanobrimonidine. This was analyzed by MTT assay. Nanobrimonidine had no negative effect on the viability of L-292 cells at all tested concentrations. **b**: *In vitro* uptake mechanism and (**c**) time-dependent uptake of nanobrimonidine: Analyses of *in vitro* uptake mechanism were performed using rhodamine-labeled nanobrimonidine into L-292 cells. The results were expressed as mean ± SD of triplicates.

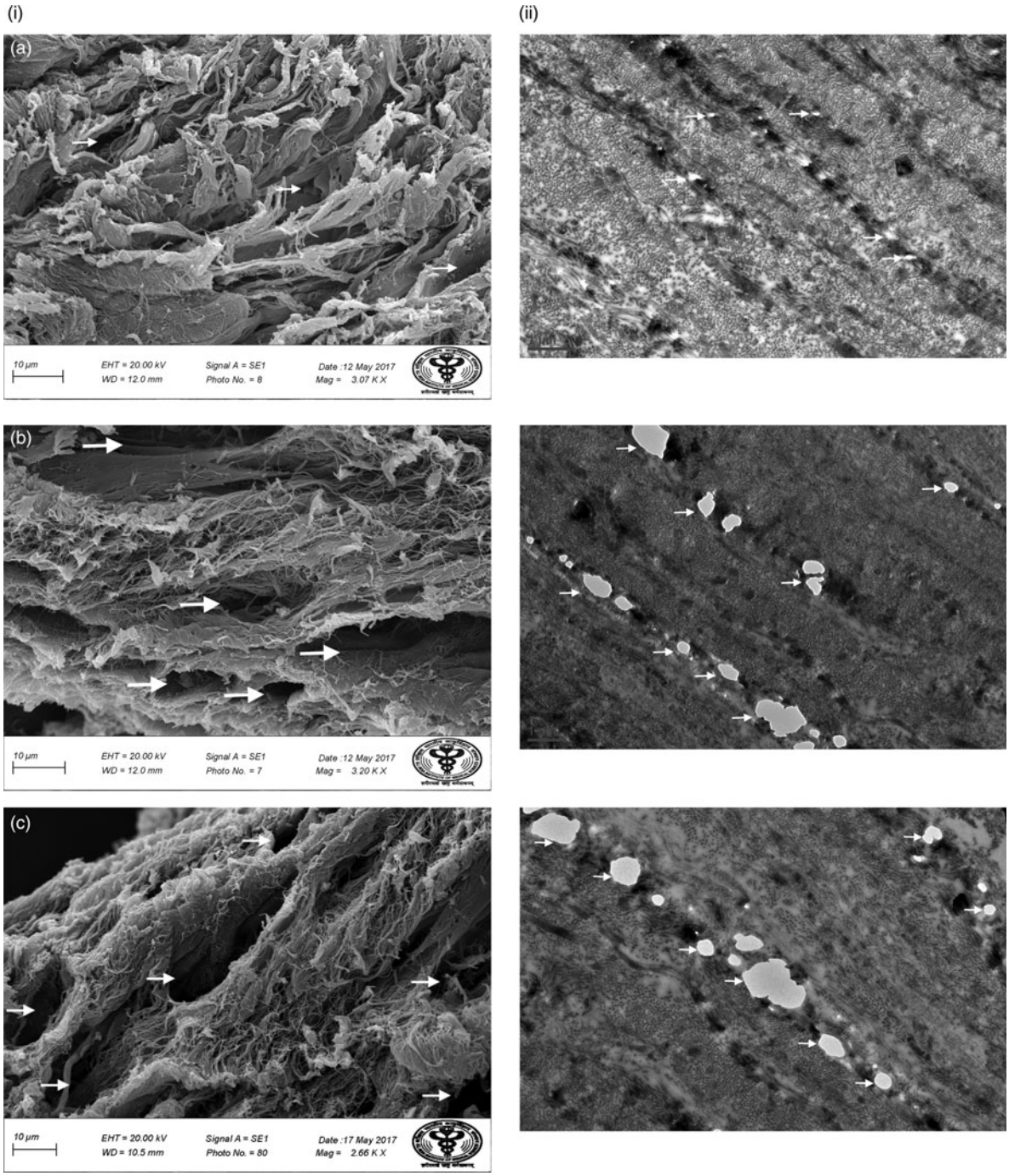

Fig. 8. Effect of various treatments of excise trabeculectomy tissue of glaucoma patients. Trabeculectomy samples (**a**) treated with naïve chitosan nanoparticles, (**b**) treated with 2.0 mg/mL free brimonidine, and (**c**) treated with nanobrimonidine of 10 mg/mL equivalent to 0.2 mg/mL of brimonidine for 24 h in DMEM. The images were taken on (i) the scanning electron microscope after fixation, dehydration, critical point drying, and sputter coating as well as (ii) the transmission electron microscope after fixation, dehydration, embedding, and ultra-sectioned (70 nm) of 24 h treated trabeculectomy sample.

under physiological condition did not show any toxic effects on cell viability, as well as proliferation, after 24 h incubation (Fig. 7a). The CyQUANT assay also showed no effect on the cellular proliferation. Thus, it is evident that nanobrimonidine does not have any dose-dependent cellular toxicity up to 5.0 mg/mL solution.

The time-dependent uptake of rhodamine-labeled nanobrimonidine by L-929 cells was analyzed by flow cytometer. It was found that nearly 50% of nanobrimonidine were taken up within 3.0 h of exposure in the medium (Fig. 7b). The *in vitro* study suggested that nanobrimonidine was primarily taken up by endocytosis. The endocytic inhibitor indomethacin (10.0 µg/mL) prevented the cellular uptake up to 50% (Fig. 7c) suggesting a caveolae-mediated endocytosis pathway to internalize into the L-929 cells.

Effect of Nanobrimonidine Treated Ex vivo *Trabeculectomy Tissue*

In advanced stages of open-angle glaucoma, the trabecular meshwork and nearby tissue of conjunctiva were excised (trabeculectomy).

The tissue from each patient was dissected into six parts in sterile condition keeping the trabecular meshwork in each part. Viability and physiological conditions of the tissue were maintained to provide the natural condition for the action of nanobrimonidine on the patient's tissue. In the scanning electron microscope, the brimonidine- and nanobrimonidine-treated tissues showed wider openings in comparison with naïve US CS NP-treated tissue (Fig. 8). Similarly, the openings of the trabecular meshwork in the TEM were wider in brimonidine- and nanobrimonidine-treated tissues as compared with naïve US CS NPs (Fig. 8). These provide an indirect confirmation that nanobrimonidine has better potential for the opening of the trabecular meshwork than that of free brimonidine. Nanobrimonidine is also more effective at ten-times lower concentration (0.2 mg/mL) than the free brimonidine (2 mg/mL), with only 33% release in 24 h. The better functionality of nanobrimonidine could be due to better penetration, EPR, and drug-releasing capability.

Summary or Conclusions

Nanobrimonidine has the potential to be used for open-angle glaucoma due to its ultra-small size (28 nm), higher drug loading capacity, stability, longer controlled release, and better functions on dilation of the trabecular meshwork. We have developed a new and simple method for the synthesis of monodisperse ultra-small (28 ± 5 nm) nanobrimonidine using modified ionotropic gelation between low molecular weight deacetylated chitosan and STPP. The stability and homogeneity of these NPs were further enhanced by surface capping using pluronic F-68 to avoid aggregation during multi-round lyophilization and re-suspension. The average zeta potential of nanobrimonidine (+37 eV) is very important for achieving the functional stability. The encapsulation efficiency was 39% and the particles were stable for months after freeze-drying. *In vitro* release study revealed that the burst release occurred in 0.5 h and complete release in 100 h. These particles showed no cytotoxicity with concentrations up to 5.0 mg/mL by MTT and CyQUANT assay. The internalization of nanobrimonidine showed the maximum uptake through receptor-mediated endocytosis pathway. The developed nanobrimonidine has good potential for the dilation of trabeculectomy tissue of glaucoma patients.

Supplementary material. The supplementary material for this article can be found at https://doi.org/10.1017/S1431927619000448

Acknowledgments. The grant received from AIIMS as Intramural Research Grants No. F. 8-419/A-419/2016/RS is greatly acknowledged. The electron microscopy imaging work done at SAIF AIIMS New Delhi and the work of Dr. Pavan Sunkireddy for ultra-small chitosan nanoparticles synthesis is also acknowledged.

References

Aburahma MH & Mahmoud AA (2011). Biodegradable ocular inserts for sustained delivery of brimonidine tartarate: Preparation and *in vitro/in vivo* evaluation. *AAPS PharmSciTech* **12**(4), 1335–1347.

Acheampong AA, Small D, Baumgarten V, Welty D & Tang-Liu D (2002). Formulation effects on ocular absorption of brimonidine in rabbit eyes. *J Ocul Pharmacol Ther* **18**(4), 325–337.

Agnihotri SA, Mallikarjuna NN & Aminabhavi TM (2004). Recent advances on chitosan-based micro- and nanoparticles in drug delivery. *J Control Release* **100**(1), 5–28.

Aksungur P, Demirbilek M, Denkbas EB, Vandervoort J, Ludwig A & Unlu N (2011). Development and characterization of cyclosporine A loaded nanoparticles for ocular drug delivery: Cellular toxicity, uptake, and kinetic studies. *J Control Release* **151**(3), 286–294.

Almeida H, Amaral MH, Lobao P & Sousa Lobo JM (2013). Applications of poloxamers in ophthalmic pharmaceutical formulations: An overview. *Expert Opin Drug Deliv* **10**(9), 1223–1237.

Almeida H, Amaral MH, Lobao P & Lobo JM (2014). *In situ* gelling systems: A strategy to improve the bioavailability of ophthalmic pharmaceutical formulations. *Drug Discov Today* **19**(4), 400–412.

Alonso MJ & Sanchez A (2003). The potential of chitosan in ocular drug delivery. *J Pharm Pharmacol* **55**(11), 1451–1463.

Anderberg EK, Bisrat M & Nyström C (1988). Physiochemical aspects of drug release. VII. The effect of surfactant concentration and drug particle size on solubility and dissolution rate of felodipine, a sparingly soluble drug. *Int J Pharm* **47**(1–3), 67–77.

Banerjee T, Mitra S, Kumar Singh A, Kumar Sharma R & Maitra A (2002). Preparation, characterization and biodistribution of ultrafine chitosan nanoparticles. *Int J Pharm* **243**(1–2), 93–105.

Binks BP & Lumsdon SO (2001). Pickering emulsions stabilized by monodispersed latex particles: Effects of particle size. *Langmuir* **17**(15), 4540–4547.

Bonferoni MC, Sandri G, Rossi S, Ferrari F & Caramella C (2009). Chitosan and its salts for mucosal and transmucosal delivery. *Expert Opin Drug Deliv* **6**(9), 923–939.

Bowman RJ, Cope J & Nischal KK (2004). Ocular and systemic side effects of brimonidine 0.2% eye drops (Alphagan) in children. *Eye (Lond)* **18**(1), 24–26.

Calvo P, Remu án-López C, Vila-Jato JL & Alonso MJ (1997). Novel hydrophilic chitosan–polyethylene oxide nanoparticles as protein carriers. *J Appl Polym Sci* **63**, 125–132.

Cantor LB (2006). Brimonidine in the treatment of glaucoma and ocular hypertension. *Ther Clin Risk Manag* **2**(4), 337–346.

Chen F, Zhang ZR & Huang Y (2007). Evaluation and modification of N-trimethyl chitosan chloride nanoparticles as protein carriers. *Int J Pharm* **336**(1), 166–173.

Cho IS, Park CG, Huh BK, Cho MO, Khatun Z, Li Z, Kang SW, Choy YB & Huh KM (2016). Thermosensitive hexanoyl glycol chitosan-based ocular delivery system for glaucoma therapy. *Acta Biomater* **39**, 124–132.

De TK, Rodman DJ, Holm BA, Prasad PN & Bergey EJ (2003). Brimonidine formulation in polyacrylic acid nanoparticles for ophthalmic delivery. *J Microencapsul* **20**(3), 361–374.

De Campos AM, Sanchez A & Alonso MJ (2001). Chitosan nanoparticles: A new vehicle for the improvement of the delivery of drugs to the ocular surface. Application to cyclosporin A. *Int J Pharm* **224**(1–2), 159–168.

de Campos AM, Diebold Y, Carvalho EL, Sanchez A & Alonso MJ (2004). Chitosan nanoparticles as new ocular drug delivery systems: *In vitro* stability, *in vivo* fate, and cellular toxicity. *Pharm Res* **21**(5), 803–810.

de la Fuente M, Seijo B & Alonso MJ (2008). Novel hyaluronic acid-chitosan nanoparticles for ocular gene therapy. *Invest Ophthalmol Vis Sci* **49**(5), 2016–2024.

Elzatahry AA & Eldin MSM (2008). Preparation and characterization of metronidazole-loaded chitosan nanoparticles for drug delivery application. *Polym Adv Technol* **19**(12), 1787–1791.

Fan W, Yan W, Xu Z & Ni H (2012). Formation mechanism of monodisperse, low molecular weight chitosan nanoparticles by ionic gelation technique. *Colloids Surf B Biointerfaces* **90**, 21–27.

Hagens WI, Oomen AG, de Jong WH, Cassee FR & Sips AJ (2007). What do we (need to) know about the kinetic properties of nanoparticles in the body? *Regul Toxicol Pharmacol* **49**(3), 217–229.

Ibrahim MM, Abd-Elgawad AH, Soliman OA & Jablonski MM (2015). Natural bioadhesive biodegradable nanoparticle-based topical ophthalmic formulations for management of glaucoma. *Transl Vis Sci Technol* **4**(3), 12.

Jarvinen K, Jarvinen T & Urtti A (1995). Ocular absorption following topical delivery. *Adv Drug Deliv Rev* **16**, 3–19.

Kim SN, Ko SA, Park CG, Lee SH, Huh BK, Park YH, Kim YK, Ha A, Park KH & Choy YB (2018). Amino-functionalized mesoporous silica particles for ocular delivery of brimonidine. *Mol Pharm* **15**(8), 3143–3152.

Lehr CM, Bowstra JA, Schacht EH & Juginger HE (1992). *In vitro* evaluation of mucoadhesive properties of chitosan and some others natural polymers. *Int J Pharm* **78**, 43–48.

Luo Q, Zhao J, Zhang X & Pan W (2011). Nanostructured lipid carrier (NLC) coated with chitosan oligosaccharides and its potential use in ocular drug delivery system. *Int J Pharm* **403**(1–2), 185–191.

Maiti S, Paul S, Mondol R, Ray S & Sa B (2011). Nanovesicular formulation of brimonidine tartrate for the management of glaucoma: *In vitro* and *in vivo* evaluation. *AAPS PharmSciTech* **12**(2), 755–763.

Malhotra M, Kulamarva A, Sebak S, Paul A, Bhathena J, Mirzaei M & Prakash S (2009). Ultrafine chitosan nanoparticles as an efficient nucleic acid delivery system targeting neuronal cells. *Drug Dev Ind Pharm* **35**(6), 719–726.

Motwani SK, Chopra S, Talegaonkar S, Kohli K, Ahmad FJ & Khar RK (2008). Chitosan-sodium alginate nanoparticles as submicroscopic reservoirs for ocular delivery: Formulation, optimisation and *in vitro* characterisation. *Eur J Pharm Biopharm* **68**(3), 513–525.

Mundada AS & Avari JG (2009). *In situ* gelling polymers in ocular drug delivery systems: A review. *Crit Rev Ther Drug Carrier Syst* **26**(1), 85–118.

Natarajan JV, Darwitan A, Barathi VA, Ang M, Htoon HM, Boey F, Tam KC, Wong TT & Venkatraman SS (2014). Sustained drug release in nanomedicine: A long-acting nanocarrier-based formulation for glaucoma. *ACS Nano* **8**(1), 419–429.

Newton MJ & Rimple (2018) Impact of ocular compatible Lipoids and Castor oil in fabrication of brimonidine tartrate nanoemulsions by 33 full factorial design. *Recent Pat Inflamm Allergy Drug Discov*.

Paolicelli P, de la Fuente M, Sanchez A, Seijo B & Alonso MJ (2009). Chitosan nanoparticles for drug delivery to the eye. *Expert Opin Drug Deliv* **6**(3), 239–253.

Prabhu P, Nitish KR, Koland M, Harish N, Vijayanarayan K, Dhondge G & Charyulu R (2010). Preparation and evaluation of nano-vesicles of brimonidine tartrate as an ocular drug delivery system. *J Young Pharm* **2**(4), 356–361.

Qun G & Ajun W (2006). Effects of molecular weight, degree of acetylation and ionic strength on surface tension of chitosan in dilute solution. *Carbohydr Polym* **64**, 29–36.

Santra S (2010). Chitosan-based nanoparticles and methods for making and using the same. In *20110158901*, US, O. F. (Ed.), USA.

Santra S & Tallury P (2011). Ultra-small chitosan nanoparticles useful as bioimaging agents and methods of making same. FSU (Ed.), USA: US20110021745A1.

Shahrouz T, Seyedali M, Mehdi M & Hossein D (2014). Development of ultrasmall chitosan/succinyl β-cyclodextrin nanoparticles as a sustained protein-delivery system. *J Appl Polym Sci* **131**(1), 39648–39648.

Shang L, Nienhaus K & Nienhaus GU (2014). Engineered nanoparticles interacting with cells: Size matters. *J Nanobiotechnology* **12**, 5.

Shi S, Fliss BC, Gu Z, Zhu Y, Hong H, Valdovinos HF, Hernandez R, Goel S, Luo H, Chen F, Barnhart TE, Nickles RJ, Xu ZP & Cai W (2015). Chelator-free labeling of layered double hydroxide nanoparticles for *in vivo* PET imaging. *Sci Rep* **5**, 16930.

Singh KH & Shinde UA (2011). Chitosan nanoparticles for controlled delivery of brimonidine tartrate to the ocular membrane. *Pharmazie* **66**(8), 594–599.

Sunkireddy P, Kanwar RK, Ram J & Kanwar JR (2016). Ultra-small algal chitosan ocular nanoparticles with iron-binding milk protein prevents the toxic effects of carbendazim pesticide. *Nanomedicine (Lond)* **11**(5), 495–511.

Tallury P, Kar S, Bamrungsap S, Huang YF, Tan W & Santra S (2009). Ultra-small water-dispersible fluorescent chitosan nanoparticles: Synthesis, characterization and specific targeting. *Chem Commun* **0**(17), 2347–2349.

Tang S, Huang Z, Zhang H, Wang Y, Hu Q & Jiang H (2014). Design and formulation of trimethylated chitosan-graft-poly(epsilon-caprolactone) nanoparticles used for gene delivery. *Carbohydr Polym* **101**, 104–112.

Wang X, Chi N & Tang X (2008). Preparation of estradiol chitosan nanoparticles for improving nasal absorption and brain targeting. *Eur J Pharm Biopharm* **70**(3), 735–740.

Wu Y, Yang W, Wang C, Hu J & Fu S (2005). Chitosan nanoparticles as a novel delivery system for ammonium glycyrrhizinate. *Int J Pharm* **295** (1–2), 235–245.

Yadav SC, Sunkireddy P, Tripathi C & Adholeya A (2013). Novel chitosan based nanoparticles/ultra nanoparticles and method for the preparation of same. In *IN 3060/DEL/2013*, India (Ed.), India.

Yang H, Tyagi P, Kadam RS, Holden CA & Kompella UB (2012). Hybrid dendrimer hydrogel/PLGA nanoparticle platform sustains drug delivery for one week and antiglaucoma effects for four days following one-time topical administration. *ACS Nano* **6**(9), 7595–7606.